

Search for Large Extra Dimensions in Final States Containing One Photon or Jet and Large Missing Transverse Energy Produced in $p\bar{p}$ Collisions at $\sqrt{s} = 1.96$ TeV

T. Aaltonen,²⁴ J. Adelman,¹⁴ T. Akimoto,⁵⁶ M. G. Albrow,¹⁸ B. Álvarez González,¹² S. Amerio,^{44a,44b} D. Amidei,³⁵ A. Anastassov,³⁹ A. Annovi,²⁰ J. Antos,¹⁵ G. Apollinari,¹⁸ A. Apresyan,⁴⁹ T. Arisawa,⁵⁸ A. Artikov,¹⁶ W. Ashmanskas,¹⁸ A. Attal,⁴ A. Aurisano,⁵⁴ F. Azfar,⁴³ P. Azzurri,^{47a,47d} W. Badgett,¹⁸ A. Barbaro-Galtieri,²⁹ V. E. Barnes,⁴⁹ B. A. Barnett,²⁶ V. Bartsch,³¹ G. Bauer,³³ P.-H. Beauchemin,³⁴ F. Bedeschi,^{47a} P. Bednar,¹⁵ D. Beecher,³¹ S. Behari,²⁶ G. Bellettini,^{47a,47b} J. Bellinger,⁶⁰ D. Benjamin,¹⁷ A. Beretvas,¹⁸ J. Beringer,²⁹ A. Bhatti,⁵¹ M. Binkley,¹⁸ D. Bisello,^{44a,44b} I. Bizjak,³¹ R. E. Blair,² C. Blocker,⁷ B. Blumenfeld,²⁶ A. Bocci,¹⁷ A. Bodek,⁵⁰ V. Boisvert,⁵⁰ G. Bolla,⁴⁹ D. Bortoletto,⁴⁹ J. Boudreau,⁴⁸ A. Boveia,¹¹ B. Brau,¹¹ A. Bridgeman,²⁵ L. Brigliadori,^{44a} C. Bromberg,³⁶ E. Brubaker,¹⁴ J. Budagov,¹⁶ H. S. Budd,⁵⁰ S. Budd,²⁵ K. Burkett,¹⁸ G. Busetto,^{44a,44b} P. Bussey,^{22,r} A. Buzatu,³⁴ K. L. Byrum,² S. Cabrera,^{17,q} C. Calancha,³² M. Campanelli,³⁶ M. Campbell,³⁵ F. Canelli,¹⁸ A. Canepa,⁴⁶ D. Carlsmith,⁶⁰ R. Carosi,^{47a} S. Carrillo,^{19,h} S. Carron,³⁴ B. Casal,¹² M. Casarsa,¹⁸ A. Castro,^{6a,6b} P. Catastini,^{47a,47c} D. Cauz,^{55a,55b} V. Cavaliere,^{47a,47c} M. Cavalli-Sforza,⁴ A. Cerri,²⁹ L. Cerrito,^{31,o} S. H. Chang,²⁸ Y. C. Chen,¹ M. Chertok,⁸ G. Chiarelli,^{47a} G. Chlachidze,¹⁸ F. Chlebana,¹⁸ K. Cho,²⁸ D. Chokheli,¹⁶ J. P. Chou,²³ G. Choudalakis,³³ S. H. Chuang,⁵³ K. Chung,¹³ W. H. Chung,⁶⁰ Y. S. Chung,⁵⁰ C. I. Ciobanu,⁴⁵ M. A. Ciocci,^{47a,47c} A. Clark,²¹ D. Clark,⁷ G. Compostella,^{44a} M. E. Convery,¹⁸ J. Conway,⁸ K. Copic,³⁵ M. Cordelli,²⁰ G. Cortiana,^{44a,44b} D. J. Cox,⁸ F. Crescioli,^{47a,47b} C. Cuenca Almenar,^{8,q} J. Cuevas,^{12,n} R. Culbertson,¹⁸ J. C. Cully,³⁵ D. Dagenhart,¹⁸ M. Datta,¹⁸ T. Davies,²² P. de Barbaro,⁵⁰ S. De Cecco,^{52a} A. Deisher,²⁹ G. De Lorenzo,⁴ M. Dell'Orso,^{47a,47b} C. Deluca,⁴ L. Demortier,⁵¹ J. Deng,¹⁷ M. Deninno,^{6a} P. F. Derwent,¹⁸ G. P. di Giovanni,⁴⁵ C. Dionisi,^{52a,52b} B. Di Ruzza,^{55a,55b} J. R. Dittmann,⁵ M. D'Onofrio,⁴ S. Donati,^{47a,47b} P. Dong,⁹ J. Donini,^{44a} T. Dorigo,^{44a} S. Dube,⁵³ J. Efron,⁴⁰ A. Elagin,⁵⁴ R. Erbacher,⁸ D. Errede,²⁵ S. Errede,²⁵ R. Eusebi,¹⁸ H. C. Fang,²⁹ S. Farrington,⁴³ W. T. Fedorko,¹⁴ R. G. Feild,⁶¹ M. Feindt,²⁷ J. P. Fernandez,³² C. Ferrazza,^{47a,47d} R. Field,¹⁹ G. Flanagan,⁴⁹ R. Forrest,⁸ M. Franklin,²³ J. C. Freeman,¹⁸ I. Furic,¹⁹ M. Gallinaro,^{52a} J. Galyardt,¹³ F. Garbersson,¹¹ J. E. Garcia,^{47a} A. F. Garfinkel,⁴⁹ K. Genser,¹⁸ H. Gerberich,²⁵ D. Gerdes,³⁵ A. Gessler,²⁷ S. Giagu,^{52a,52b} V. Giakoumopoulou,³ P. Giannetti,^{47a} K. Gibson,⁴⁸ J. L. Gimmell,⁵⁰ C. M. Ginsburg,¹⁸ N. Giokaris,³ M. Giordani,^{55a,55b} P. Giromini,²⁰ M. Giunta,^{47a,47b} G. Giurgiu,²⁶ V. Glagolev,¹⁶ D. Glenzinski,¹⁸ M. Gold,³⁸ N. Goldschmidt,¹⁹ A. Golossanov,¹⁸ G. Gomez,¹² G. Gomez-Ceballos,³³ M. Goncharov,⁵⁴ O. González,³² I. Gorelov,³⁸ A. T. Goshaw,¹⁷ K. Goulianos,⁵¹ A. Gresele,^{44a,44b} S. Grinstein,²³ C. Grosso-Pilcher,¹⁴ R. C. Group,¹⁸ U. Grundler,²⁵ J. Guimaraes da Costa,²³ Z. Gunay-Unalan,³⁶ C. Haber,²⁹ K. Hahn,³³ S. R. Hahn,¹⁸ E. Halkiadakis,⁵³ B.-Y. Han,⁵⁰ J. Y. Han,⁵⁰ R. Handler,⁶⁰ F. Happacher,²⁰ K. Hara,⁵⁶ D. Hare,⁵³ M. Hare,⁵⁷ S. Harper,⁴³ R. F. Harr,⁵⁹ R. M. Harris,¹⁸ M. Hartz,⁴⁸ K. Hatakeyama,⁵¹ J. Hauser,⁹ C. Hays,⁴³ M. Heck,²⁷ A. Heijboer,⁴⁶ B. Heinemann,²⁹ J. Heinrich,⁴⁶ C. Henderson,³³ M. Herndon,⁶⁰ J. Heuser,²⁷ S. Hewamanage,⁵ D. Hidas,¹⁷ C. S. Hill,^{11,d} D. Hirschbuehl,²⁷ A. Hocker,¹⁸ S. Hou,¹ M. Houlden,³⁰ S.-C. Hsu,¹⁰ B. T. Huffman,⁴³ R. E. Hughes,⁴⁰ U. Husemann,⁶¹ J. Huston,³⁶ J. Incandela,¹¹ G. Introzzi,^{47a} M. Iori,^{52a,52b} A. Ivanov,⁸ E. James,¹⁸ B. Jayatilaka,¹⁷ E. J. Jeon,²⁸ M. K. Jha,^{6a} S. Jindariani,¹⁸ W. Johnson,⁸ M. Jones,⁴⁹ K. K. Joo,²⁸ S. Y. Jun,¹³ J. E. Jung,²⁸ T. R. Junk,¹⁸ T. Kamon,⁵⁴ D. Kar,¹⁹ P. E. Karchin,⁵⁹ Y. Kato,⁴² R. Kephart,¹⁸ J. Keung,⁴⁶ V. Khotilovich,⁵⁴ B. Kilminster,⁴⁰ D. H. Kim,²⁸ H. S. Kim,²⁸ J. E. Kim,²⁸ M. J. Kim,²⁰ S. B. Kim,²⁸ S. H. Kim,⁵⁶ Y. K. Kim,¹⁴ N. Kimura,⁵⁶ L. Kirsch,⁷ S. Klimentenko,¹⁹ B. Knuteson,³³ B. R. Ko,¹⁷ S. A. Koay,¹¹ K. Kondo,⁵⁸ D. J. Kong,²⁸ J. Konigsberg,¹⁹ A. Korytov,¹⁹ A. V. Kotwal,¹⁷ M. Kreps,²⁷ J. Kroll,⁴⁶ D. Krop,¹⁴ N. Krumnack,⁵ M. Kruse,¹⁷ V. Krutelyov,¹¹ T. Kubo,⁵⁶ T. Kuhr,²⁷ N. P. Kulkarni,⁵⁹ M. Kurata,⁵⁶ Y. Kusakabe,⁵⁸ S. Kwang,¹⁴ A. T. Laasanen,⁴⁹ S. Lami,^{47a} S. Lammel,¹⁸ M. Lancaster,³¹ R. L. Lander,⁸ K. Lannon,⁴⁰ A. Lath,⁵³ G. Latino,^{47a,47c} I. Lazzizzera,^{44a,44b} T. LeCompte,² E. Lee,⁵⁴ H. S. Lee,¹⁴ S. W. Lee,^{54,p} S. Leone,^{47a} J. D. Lewis,¹⁸ C. S. Lin,²⁹ J. Linacre,⁴³ M. Lindgren,¹⁸ E. Lipeles,¹⁰ A. Lister,⁸ D. O. Litvintsev,¹⁸ C. Liu,⁴⁸ T. Liu,¹⁸ N. S. Lockyer,⁴⁶ A. Loginov,⁶¹ M. Loretì,^{44a,44b} L. Lovas,¹⁵ R.-S. Lu,¹ D. Lucchesi,^{44a,44b} J. Lueck,²⁷ C. Luci,^{52a,52b} P. Lujan,²⁹ P. Lukens,¹⁸ G. Lungu,⁵¹ L. Lyons,⁴³ J. Lys,²⁹ R. Lysak,¹⁵ E. Lytken,⁴⁹ P. Mack,²⁷ D. MacQueen,³⁴ R. Madrak,¹⁸ K. Maeshima,¹⁸ K. Makhoul,³³ T. Maki,²⁴ P. Maksimovic,²⁶ S. Malde,⁴³ S. Malik,³¹ G. Manca,^{30,s} A. Manousakis-Katsikakis,³ F. Margaroli,⁴⁹ C. Marino,²⁷ C. P. Marino,²⁵ A. Martin,⁶¹ V. Martin,^{22,j} M. Martínez,⁴ R. Martínez-Ballarín,³² T. Maruyama,⁵⁶ P. Mastrandrea,^{52a} T. Masubuchi,⁵⁶ M. E. Mattson,⁵⁹ P. Mazzanti,^{6a} K. S. McFarland,⁵⁰ P. McIntyre,⁵⁴ R. McNulty,^{30,i} A. Mehta,³⁰ P. Mehtala,²⁴ A. Menzione,^{47a} P. Merkel,⁴⁹ C. Mesropian,⁵¹ T. Miao,¹⁸ N. Miladinovic,⁷ R. Miller,³⁶ C. Mills,²³ M. Milnik,²⁷ A. Mitra,¹ G. Mitselmakher,¹⁹ H. Miyake,⁵⁶ N. Moggi,^{6a} C. S. Moon,²⁸ R. Moore,¹⁸ M. J. Morello,^{47a,47b} J. Morlok,²⁷ P. Movilla Fernandez,¹⁸ J. Mülmenstädt,²⁹ A. Mukherjee,¹⁸ Th. Müller,²⁷ R. Mumford,²⁶

P. Murat,¹⁸ M. Mussini,^{6a,6b} J. Nachtman,¹⁸ Y. Nagai,⁵⁶ A. Nagano,⁵⁶ J. Naganoma,⁵⁸ K. Nakamura,⁵⁶ I. Nakano,⁴¹ A. Napier,⁵⁷ V. Necula,¹⁷ C. Neu,⁴⁶ M. S. Neubauer,²⁵ J. Nielsen,^{29,f} L. Nodulman,² M. Norman,¹⁰ O. Normiella,²⁵ E. Nurse,³¹ L. Oakes,⁴³ S. H. Oh,¹⁷ Y. D. Oh,²⁸ I. Oksuzian,¹⁹ T. Okusawa,⁴² R. Orava,²⁴ K. Osterberg,²⁴ S. Pagan Griso,^{44a,44b} C. Pagliarone,^{47a} E. Palencia,¹⁸ V. Papadimitriou,¹⁸ A. Papaikonomou,²⁷ A. A. Paramonov,¹⁴ B. Parks,⁴⁰ S. Pashapour,³⁴ J. Patrick,¹⁸ G. Pauletta,^{55a,55b} M. Paulini,¹³ C. Paus,³³ D. E. Pellett,⁸ A. Penzo,^{55a} T. J. Phillips,¹⁷ G. Piacentino,^{47a} E. Pianori,⁴⁶ L. Pinera,¹⁹ K. Pitts,²⁵ C. Plager,⁹ L. Pondrom,⁶⁰ O. Poukhov,^{16,a} N. Pounder,⁴³ F. Prakoshyn,¹⁶ A. Pronko,¹⁸ J. Proudfoot,² F. Ptohos,^{18,h} E. Pueschel,¹³ G. Punzi,^{47a,47b} J. Pursley,⁶⁰ J. Rademacker,^{43,d} A. Rahaman,⁴⁸ V. Ramakrishnan,⁶⁰ N. Ranjan,⁴⁹ I. Redondo,³² B. Reiser,¹⁸ V. Rekovic,³⁸ P. Renton,⁴³ M. Rescigno,^{52a} S. Richter,²⁷ F. Rimondi,^{6a,6b} L. Ristori,^{47a} A. Robson,²² T. Rodrigo,¹² T. Rodriguez,⁴⁶ E. Rogers,²⁵ S. Rolli,⁵⁷ R. Roser,¹⁸ M. Rossi,^{55a} R. Rossin,¹¹ P. Roy,³⁴ A. Ruiz,¹² J. Russ,¹³ V. Rusu,¹⁸ H. Saarikko,²⁴ A. Safonov,⁵⁴ W. K. Sakumoto,⁵⁰ O. Saltó,⁴ L. Santi,^{55a,55b} S. Sarkar,^{52a,52b} L. Sartori,^{47a} K. Sato,¹⁸ P. Savard,³⁴ A. Savoy-Navarro,⁴⁵ T. Scheidle,²⁷ P. Schlabach,¹⁸ A. Schmidt,²⁷ E. E. Schmidt,¹⁸ M. A. Schmidt,¹⁴ M. P. Schmidt,^{61,a} M. Schmitt,³⁹ T. Schwarz,⁸ L. Scodellaro,¹² A. L. Scott,¹¹ A. Scribano,^{47a,47c} F. Scuri,^{47a} A. Sedov,⁴⁹ S. Seidel,³⁸ Y. Seiya,⁴² A. Semenov,¹⁶ L. Sexton-Kennedy,¹⁸ A. Sfyrila,²¹ S. Z. Shalhout,⁵⁹ T. Shears,³⁰ P. F. Shepard,⁴⁸ D. Sherman,²³ M. Shimojima,^{56,m} S. Shiraishi,¹⁴ M. Shochet,¹⁴ Y. Shon,⁶⁰ I. Shreyber,³⁷ A. Sidoti,^{47a} P. Sinervo,³⁴ A. Sisakyan,¹⁶ A. J. Slaughter,¹⁸ J. Slaunwhite,⁴⁰ K. Sliwa,⁵⁷ J. R. Smith,⁸ F. D. Snider,¹⁸ R. Snihur,³⁴ A. Soha,⁸ S. Somalwar,⁵³ V. Sorin,³⁶ J. Spalding,¹⁸ T. Spreitzer,³⁴ P. Squillacioti,^{47a,47c} M. Stanitzki,⁶¹ R. St. Denis,²² B. Stelzer,⁹ O. Stelzer-Chilton,⁴³ D. Stentz,³⁹ J. Strologas,³⁸ D. Stuart,¹¹ J. S. Suh,²⁸ A. Sukhanov,¹⁹ I. Suslov,¹⁶ T. Suzuki,⁵⁶ A. Taffard,^{25,e} R. Takashima,⁴¹ Y. Takeuchi,⁵⁶ R. Tanaka,⁴¹ M. Tecchio,³⁵ P. K. Teng,¹ K. Terashi,⁵¹ J. Thom,^{18,g} A. S. Thompson,²² G. A. Thompson,²⁵ E. Thomson,⁴⁶ P. Tipton,⁶¹ V. Tiwari,¹³ S. Tkaczyk,¹⁸ D. Toback,⁵⁴ S. Tokar,¹⁵ K. Tollefson,³⁶ T. Tomura,⁵⁶ D. Tonelli,¹⁸ S. Torre,²⁰ D. Torretta,¹⁸ P. Totaro,^{55a,55b} S. Tourneur,⁴⁵ Y. Tu,⁴⁶ N. Turini,^{47a,47c} F. Ukegawa,⁵⁶ S. Vallecorsa,²¹ N. van Remortel,^{24,b} A. Varganov,³⁵ E. Vataga,^{47a,47d} F. Vázquez,^{19,k} G. Velev,¹⁸ C. Vellidis,³ V. Veszpremi,⁴⁹ M. Vidal,³² R. Vidal,¹⁸ I. Vila,¹² R. Vilar,¹² T. Vine,³¹ M. Vogel,³⁸ I. Volobouev,^{29,p} G. Volpi,^{47a,47b} F. Würthwein,¹⁰ P. Wagner,² R. G. Wagner,² R. L. Wagner,¹⁸ J. Wagner-Kuhr,²⁷ W. Wagner,²⁷ T. Wakisaka,⁴² R. Wallny,⁹ S. M. Wang,¹ A. Warburton,³⁴ D. Waters,³¹ M. Weinberger,⁵⁴ W. C. Wester III,¹⁸ B. Whitehouse,⁵⁷ D. Whiteson,^{46,e} A. B. Wicklund,² E. Wicklund,¹⁸ G. Williams,³⁴ H. H. Williams,⁴⁶ P. Wilson,¹⁸ B. L. Winer,⁴⁰ P. Wittich,^{18,g} S. Wolbers,¹⁸ C. Wolfe,¹⁴ T. Wright,³⁵ X. Wu,²¹ S. M. Wynne,³⁰ S. Xie,³³ A. Yagil,¹⁰ K. Yamamoto,⁴² J. Yamaoka,⁵³ U. K. Yang,^{14,1} Y. C. Yang,²⁸ W. M. Yao,²⁹ G. P. Yeh,¹⁸ J. Yoh,¹⁸ K. Yorita,¹⁴ T. Yoshida,⁴² G. B. Yu,⁵⁰ I. Yu,²⁸ S. S. Yu,¹⁸ J. C. Yun,¹⁸ L. Zanello,^{52a,52b} A. Zanetti,^{55a} I. Zaw,²³ X. Zhang,²⁵ Y. Zheng,^{9,c} and S. Zucchelli^{6a,6b}

(CDF Collaboration)

¹*Institute of Physics, Academia Sinica, Taipei, Taiwan 11529, Republic of China*²*Argonne National Laboratory, Argonne, Illinois 60439, USA*³*University of Athens, 157 71 Athens, Greece*⁴*Institut de Física d'Altes Energies, Universitat Autònoma de Barcelona, E-08193, Bellaterra (Barcelona), Spain*⁵*Baylor University, Waco, Texas 76798, USA*^{6a}*Istituto Nazionale di Fisica Nucleare Bologna, I-40127 Bologna, Italy*^{6b}*University of Bologna, I-40127 Bologna, Italy*⁷*Brandeis University, Waltham, Massachusetts 02254, USA*⁸*University of California, Davis, Davis, California 95616, USA*⁹*University of California, Los Angeles, Los Angeles, California 90024, USA*¹⁰*University of California, San Diego, La Jolla, California 92093, USA*¹¹*University of California, Santa Barbara, Santa Barbara, California 93106, USA*¹²*Instituto de Física de Cantabria, CSIC-University of Cantabria, 39005 Santander, Spain*¹³*Carnegie Mellon University, Pittsburgh, Pennsylvania 15213, USA*¹⁴*Enrico Fermi Institute, University of Chicago, Chicago, Illinois 60637, USA*¹⁵*Comenius University, 842 48 Bratislava, Slovakia; Institute of Experimental Physics, 040 01 Kosice, Slovakia*¹⁶*Joint Institute for Nuclear Research, RU-141980 Dubna, Russia*¹⁷*Duke University, Durham, North Carolina 27708, USA*¹⁸*Fermi National Accelerator Laboratory, Batavia, Illinois 60510, USA*¹⁹*University of Florida, Gainesville, Florida 32611, USA*²⁰*Laboratori Nazionali di Frascati, Istituto Nazionale di Fisica Nucleare, I-00044 Frascati, Italy*²¹*University of Geneva, CH-1211 Geneva 4, Switzerland*²²*Glasgow University, Glasgow G12 8QQ, United Kingdom*

- ²³Harvard University, Cambridge, Massachusetts 02138, USA
- ²⁴Division of High Energy Physics, Department of Physics, University of Helsinki and Helsinki Institute of Physics, FIN-00014, Helsinki, Finland
- ²⁵University of Illinois, Urbana, Illinois 61801, USA
- ²⁶The Johns Hopkins University, Baltimore, Maryland 21218, USA
- ²⁷Institut für Experimentelle Kernphysik, Universität Karlsruhe, 76128 Karlsruhe, Germany
- ²⁸Center for High Energy Physics: Kyungpook National University, Daegu 702-701, Korea; Seoul National University, Seoul 151-742, Korea; Sungkyunkwan University, Suwon 440-746, Korea; Korea Institute of Science and Technology Information, Daejeon, 305-806, Korea; Chonnam National University, Gwangju, 500-757, Korea
- ²⁹Ernest Orlando Lawrence Berkeley National Laboratory, Berkeley, California 94720, USA
- ³⁰University of Liverpool, Liverpool L69 7ZE, United Kingdom
- ³¹University College London, London WC1E 6BT, United Kingdom
- ³²Centro de Investigaciones Energeticas Medioambientales y Tecnológicas, E-28040 Madrid, Spain
- ³³Massachusetts Institute of Technology, Cambridge, Massachusetts 02139, USA
- ³⁴Institute of Particle Physics: McGill University, Montréal, Canada H3A 2T8; and University of Toronto, Toronto, Canada M5S 1A7
- ³⁵University of Michigan, Ann Arbor, Michigan 48109, USA
- ³⁶Michigan State University, East Lansing, Michigan 48824, USA
- ³⁷Institution for Theoretical and Experimental Physics, ITEP, Moscow 117259, Russia
- ³⁸University of New Mexico, Albuquerque, New Mexico 87131, USA
- ³⁹Northwestern University, Evanston, Illinois 60208, USA
- ⁴⁰The Ohio State University, Columbus, Ohio 43210, USA
- ⁴¹Okayama University, Okayama 700-8530, Japan
- ⁴²Osaka City University, Osaka 588, Japan
- ⁴³University of Oxford, Oxford OX1 3RH, United Kingdom
- ^{44a}Istituto Nazionale di Fisica Nucleare, Sezione di Padova-Trento, I-35131 Padova, Italy
- ^{44b}University of Padova, I-35131 Padova, Italy
- ⁴⁵LPNHE, Université Pierre et Marie Curie/IN2P3-CNRS, UMR7585, Paris, F-75252, France
- ⁴⁶University of Pennsylvania, Philadelphia, Pennsylvania 19104, USA
- ^{47a}Istituto Nazionale di Fisica Nucleare Pisa, I-56127 Pisa, Italy
- ^{47b}University of Pisa, I-56127 Pisa, Italy
- ^{47c}University of Siena, I-56127 Pisa, Italy
- ^{47d}Scuola Normale Superiore, I-56127 Pisa, Italy
- ⁴⁸University of Pittsburgh, Pittsburgh, Pennsylvania 15260, USA
- ⁴⁹Purdue University, West Lafayette, Indiana 47907, USA
- ⁵⁰University of Rochester, Rochester, New York 14627, USA
- ⁵¹The Rockefeller University, New York, New York 10021, USA
- ^{52a}Istituto Nazionale di Fisica Nucleare, Sezione di Roma 1, I-00185 Roma, Italy
- ^{52b}Sapienza Università di Roma, I-00185 Roma, Italy
- ⁵³Rutgers University, Piscataway, New Jersey 08855, USA
- ⁵⁴Texas A&M University, College Station, Texas 77843, USA
- ^{55a}Istituto Nazionale di Fisica Nucleare Trieste/Udine, Italy
- ^{55b}University of Trieste/Udine, Italy
- ⁵⁶University of Tsukuba, Tsukuba, Ibaraki 305, Japan
- ⁵⁷Tufts University, Medford, Massachusetts 02155, USA
- ⁵⁸Waseda University, Tokyo 169, Japan
- ⁵⁹Wayne State University, Detroit, Michigan 48201, USA
- ⁶⁰University of Wisconsin, Madison, Wisconsin 53706, USA
- ⁶¹Yale University, New Haven, Connecticut 06520, USA
- (Received 22 July 2008; published 31 October 2008)

We present the results of searches for large extra dimensions in samples of events with large missing transverse energy \cancel{E}_T and either a photon or a jet produced in $p\bar{p}$ collisions at $\sqrt{s} = 1.96$ TeV collected with the Collider Detector at Fermilab II. For $\gamma + \cancel{E}_T$ and jet + \cancel{E}_T candidate samples corresponding to 2.0 and 1.1 fb⁻¹ of integrated luminosity, respectively, we observe good agreement with standard model expectations and obtain a combined lower limit on the fundamental parameter of the large extra dimensions model M_D as a function of the number of extra dimensions in the model.

The mass of the Higgs particle in the standard model (SM) is subject to large quantum corrections. This is attributed to the existence of two equally fundamental energy scales in nature: the scale of the electroweak interaction [$\mathcal{O}(100 \text{ GeV})$] and the scale of the gravitational interaction [$\mathcal{O}(10^{19} \text{ GeV})$]. One class of solutions to this hierarchy problem introduces new symmetries which protect physical parameters, such as the Higgs boson mass, from large quantum corrections. However, these models introduce an additional complication in that the new symmetries are required to be broken at some unknown scale and in some unknown way. An alternate approach is to reconcile the hierarchy between the electroweak and gravity (Planck) scales by introducing extra spatial dimensions.

In the large extra dimensions (LED) scenario of Arkani-Hamed, Dimopoulos, and Dvali (ADD) [1], gravity propagates in the $(4 + n)$ -dimensional “bulk” of space-time, while the other SM fields are confined to our usual four dimensions. The observed discrepancy between the size of Newton’s constant and the strength of the electroweak couplings is understood as an artifact of the four-dimensional bias of the observer. The four-dimensional Planck scale M_{Pl} is related to the fundamental $(4 + n)$ -dimensional Planck scale M_D by $M_{\text{Pl}}^2 \sim R^n M_D^{n+2}$, where n and R are the number and size of the extra dimensions, respectively. An appropriate choice of R for a given n leads to a value of M_D of the same order as that of the electroweak scale.

Although models incorporating extra dimensions do not completely solve the hierarchy problem (R has to be tuned to provide a match between the fundamental electroweak and Planck scales), their realization would provide an extraordinary and unique opportunity for direct studies of gravity at the Tevatron. In these models the graviton (G is used to denote all possible integer spin states from 0 to 2) is produced in the final states of the following interactions: $q\bar{q} \rightarrow \gamma G$, $q\bar{q} \rightarrow gG$, $qg \rightarrow qG$, and $gg \rightarrow gG$. The cross section for direct graviton production depends solely on the fundamental Planck scale M_D due to cancellation of terms proportional to M_{Pl} (the relevant graviton-parton couplings suppress the cross section by M_{Pl}^{-2} while the increased phase space volume due to the presence of the extra dimensions is proportional to $R^n \sim M_{\text{Pl}}^2/M_D^{n+2}$). Conversely, the interaction of the produced graviton with material in the detector does not benefit from the increased phase space volume effect [2]. The final state graviton will therefore pass through the detector undetected, resulting in a signature of a single jet [3] or photon accompanied by large missing transverse energy \cancel{E}_T [4]. A previous search using single high- E_T jet + \cancel{E}_T data corresponding to 368 pb^{-1} of integrated luminosity collected with the Collider Detector at Fermilab (CDF II) [5] observed no significant event excess with respect to SM expectations and placed the world’s best lower limits on M_D for the cases of five or more extra dimensions ($M_D > 0.83 \text{ TeV}$

for $n = 6$). The previous most sensitive search made at a hadron collider using the $\gamma + \cancel{E}_T$ channel was performed by the D0 Collaboration [6].

In this Letter we describe an improved search for LED based on independent analyses of single jet + \cancel{E}_T and $\gamma + \cancel{E}_T$ data samples corresponding to 1.1 and 2.0 fb^{-1} of integrated luminosity, respectively. Both analyses focused on a specific event signature and were sensitive to a broad range of new physics models. Subsequent optimization of kinematic selection criteria was done to maximize sensitivity to the LED model. The combined analysis presented here has significantly better sensitivity to LED model parameters than previous measurements. Analysis of the $\gamma + \cancel{E}_T$ data sample relies heavily on the electromagnetic shower timing system [7], which is critical in minimizing substantial cosmic ray backgrounds.

A full description of the CDF II detector can be found elsewhere [8]. Events in the $\gamma + \cancel{E}_T$ sample must satisfy the criteria at all three levels of the CDF II trigger system for a high energy electromagnetic cluster ($E_T > 25 \text{ GeV}$) in the region $|\eta| < 1.1$ and $\cancel{E}_T > 25 \text{ GeV}$. The trigger is found to be $\sim 100\%$ efficient for the final γ and \cancel{E}_T kinematic selection requirements. The highest- E_T photon candidate in the fiducial region of the calorimeter is required to pass standard photon identification cuts [9,10]. Candidate events are required to have $\cancel{E}_T > 50 \text{ GeV}$ and contain at least one central photon with $|\eta| < 1.1$ and $E_T > 50 \text{ GeV}$. To reduce $W + \text{jet}$, where the jet is misidentified as a photon, and $W + \gamma$ background events containing tracks with $p_T > 10 \text{ GeV}/c$ are vetoed. We also reject events containing jets with $E_T > 15 \text{ GeV}$ to reduce the background from $\gamma + \text{jet}$ events with large \cancel{E}_T originating from jet energy mismeasurements. In order to reduce non-collision backgrounds we require a minimum of three good quality tracks in each candidate event. The reconstructed photon is also required to be consistent in time with the $p\bar{p}$ collision and satisfy a discriminant [11] that separates photons produced in collisions from those originating from cosmic rays.

Table I shows a breakdown of the estimated SM backgrounds in the $\gamma + \cancel{E}_T$ event sample using two photon E_T requirements. Collision-produced backgrounds include the irreducible contribution from $Z\gamma \rightarrow \nu\bar{\nu}\gamma$, $W \rightarrow \ell\nu$ production where the lepton is reconstructed as a photon, as well as $W\gamma$ and $\gamma\gamma$ production where the W decay lepton or second photon is undetected. The processes containing misidentified or undetected leptons are important at low energies but less so at higher energies since a small fraction of the leptons from W decays are produced with $E_T > 90 \text{ GeV}$. The $Z\gamma$, $W \rightarrow \mu\nu$, and $W \rightarrow \tau\nu$ contributions are estimated from Monte Carlo simulation, while data-driven methods are used to estimate backgrounds for which the simulation is less reliable.

In the case of $W \rightarrow e\nu$ we rely on Monte Carlo simulation to determine the E_T dependence of the probability for

TABLE I. Number of observed events and expected SM backgrounds in the $\gamma + \cancel{E}_T$ candidate sample based on minimum photon E_T requirements of 50 and 90 GeV.

Background	$E_T^\gamma > 50$ GeV	$E_T^\gamma > 90$ GeV
$W \rightarrow e \rightarrow \gamma$	47.3 ± 5.1	2.6 ± 0.4
$W \rightarrow \mu/\tau \rightarrow \gamma$	19.1 ± 4.2	1.0 ± 0.2
$W\gamma \rightarrow \mu\gamma \rightarrow \gamma$	33.1 ± 10.2	1.7 ± 1.2
$W\gamma \rightarrow e\gamma \rightarrow \gamma$	8.0 ± 3.0	0.8 ± 0.7
$W\gamma \rightarrow \tau\gamma \rightarrow \gamma$	17.6 ± 1.6	2.5 ± 0.2
$\gamma\gamma \rightarrow \gamma$	18.9 ± 2.3	2.3 ± 0.6
Cosmic ray	36.4 ± 2.5	9.8 ± 1.3
$Z\gamma \rightarrow \nu\nu\gamma$	100.1 ± 9.5	25.6 ± 2.0
Total predicted	280.5 ± 15.7	46.3 ± 3.0
Data observed	280	40

an electron to be reconstructed as a photon. A data sample of $e\gamma$ events with small \cancel{E}_T and electron-photon invariant mass consistent with the Z boson is used to normalize the modeled E_T dependence. A similar approach is used to estimate $W\gamma$ and $\gamma\gamma$ backgrounds. The relative rate for observing only a single photon is determined from simulation, while the absolute normalization comes from the observed number of fully reconstructed events in data. For example, we estimate the $\gamma\gamma$ background by determining the ratio of diphoton events with one and two reconstructed photons from simulation and multiplying by the number of observed two photon events in data. Note that this approach also accounts for the additional contribution from $\gamma + \text{jet}$ events in cases where the original photon is lost and the jet is misidentified as a photon since the corresponding two photon events will be included in the event sample used for the normalization.

For photons with higher energies, the $Z\gamma \rightarrow \nu\nu\gamma$ background becomes increasingly dominant. To estimate this background we use a leading-order (LO) Monte Carlo simulation [12]. We determine that the LO description is adequate in the presence of our jet veto based on studies of the next-to-leading-order (NLO) version of the simulation, which indicate that the increase in the total cross section originating from the inclusion of NLO diagrams in the calculation is canceled by an equivalent decrease in acceptance due to the jet veto requirement.

Noncollision backgrounds which mimic the $\gamma + \cancel{E}_T$ signature originate from cosmic rays and particle interactions upstream of the detector. Beam-produced muons traverse the calorimeter parallel to the beam line and deposit energy in multiple calorimeter towers covering the same azimuthal range. The cuts used to remove events with this topology and the method for estimating their residual contribution to the final candidate sample are the same as those used in previous searches [13]. We predict a negligible contribution (less than one event) in our sample from noncollision backgrounds of this type.

We use the new calorimeter timing system to reduce background from cosmic rays. Photon candidates originating from cosmic rays are uncorrelated in time with collisions and therefore produce roughly flat timing distributions. The timing distribution of photons produced in collisions has a Gaussian shape with a mean of zero and standard deviation of 1.6 ns [7] which is a factor of 2.3 improvement in timing resolution over that obtained from the original system. The improved resolution translates into an equivalent reduction factor in the cosmic ray background and allows for selection of a pure cosmic photon sample to train a discriminant that further separates collision photons from those produced by cosmic rays. The discriminant provides an additional factor of 10 reduction in the cosmic ray background with no loss in signal efficiency. We estimate the residual background using photon candidates at least 20 ns out of time with the collision to predict the level of background in the timing window around the collision. Despite these improvements cosmic rays account for roughly 20% of the total background in the high photon- E_T region where we are most sensitive to new physics.

Figure 1 and Table I illustrate the agreement between the CDF II $\gamma + \cancel{E}_T$ event sample and the SM background expectation. We observe good agreement for both the low and high regions of the photon E_T spectrum.

The procedure used to analyze the jet + \cancel{E}_T sample has been described in a previous publication [5]. The kinematic requirements, determined *a priori*, used to optimize sensitivity to LED are a single jet with $E_T > 150$ GeV and $\cancel{E}_T > 120$ GeV (a second jet with $E_T < 60$ GeV is allowed to increase signal acceptance). The analysis reported here is

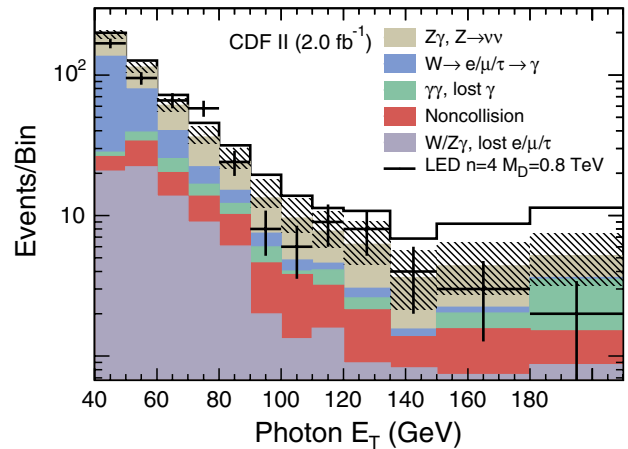


FIG. 1 (color online). Predicted (solid) and observed (crosses) photon E_T distributions for the $\gamma + \cancel{E}_T$ candidate sample. The last bin shows all events containing a photon with $E_T > 180$ GeV. The expected LED signal for the case of $n = 4$ and $M_D = 0.8$ TeV is also shown. The kinematic region above 90 GeV is used for constraining the ADD model. The hatched region indicates the total uncertainty on the combined background prediction.

TABLE II. Number of observed events and expected SM backgrounds in the jet + \cancel{E}_T candidate sample.

Background	Events
$Z \rightarrow \nu\bar{\nu}$	388 ± 30
$W \rightarrow \tau\nu$	187 ± 14
$W \rightarrow \mu\nu$	117 ± 9
$W \rightarrow e\nu$	58 ± 4
$Z \rightarrow \ell\ell$	8 ± 1
Multijet	23 ± 20
γ + jet	17 ± 5
Noncollision	10 ± 10
Total predicted	808 ± 62
Data observed	809

simply an update to the previously published analysis. The SM background estimates and the number of observed events are shown in Table II, and a comparison of the expected and observed leading jet E_T distributions is shown in Fig. 2.

Based on the observed agreement with the SM expectation in both the $\gamma + \cancel{E}_T$ and jet + \cancel{E}_T candidate samples, we proceed to set lower limits on M_D for the LED model. The limits are obtained solely from the total number of observed events in each of the samples (no kinematic shape information is incorporated). In order to estimate our sensitivity to the ADD model we simulate expected signals in both final states using the PYTHIA [14] event generator in conjunction with a GEANT [15] based detector simulation. For each extra dimension scenario we simulate event samples for M_D ranging between 0.7 and 2 TeV. In the case of the $\gamma + \cancel{E}_T$ analysis, the final kinematic selection requirements for the candidate sample are determined by optimizing the expected cross section limit without looking at the data. The jet + \cancel{E}_T analysis was done as a generic

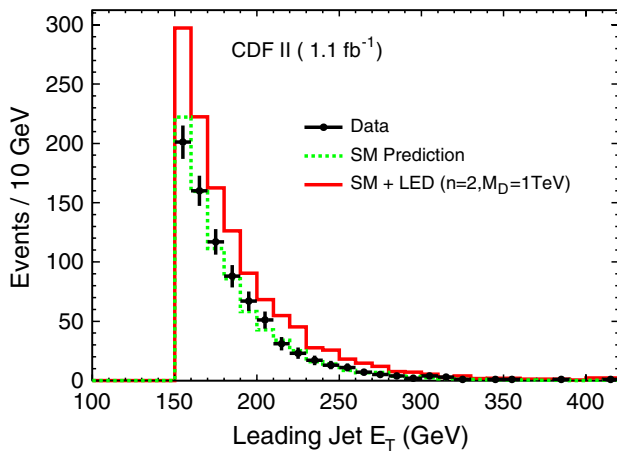


FIG. 2 (color online). Predicted and observed leading jet E_T distributions for the jet + \cancel{E}_T candidate sample. The expected LED signal contribution for the case of $n = 2$ and $M_D = 1.0$ TeV is also shown.

TABLE III. Percentage of signal events passing the candidate sample selection criteria (α) and observed 95% C.L. lower limits on the effective Planck scale in the ADD model (M_D^{obs}) in GeV/c^2 as a function of the number of extra dimensions in the model (n) for both individual and the combined analysis.

n	$\gamma + \cancel{E}_T$		jet + \cancel{E}_T		Combined M_D^{obs}
	α	M_D^{obs}	α	M_D^{obs}	
2	7.2	1080	9.9	1310	1400
3	7.2	1000	11.1	1080	1150
4	7.6	970	12.6	980	1040
5	7.3	930	12.1	910	980
6	7.2	900	12.3	880	940

search for new physics using three sets of kinematic cuts, the most sensitive of which is used here. To compute the expected 95% C.L. cross section upper limits we combine the predicted ADD signal and background estimates with systematic uncertainties on the acceptance using a Bayesian method with a flat prior [16]. The acceptance is found to be almost independent (within 2%) of the mass M_D . The total systematic uncertainties on the number of expected signal events are 5.7% and 12.4% for the $\gamma + \cancel{E}_T$ and jet + \cancel{E}_T candidate samples, respectively. The largest systematic uncertainties arise from modeling of initial or final state radiation convoluted with jet veto requirements, choice of renormalization and factorization scales, modeling of parton distribution functions, modeling of the jet energy scale (jet + \cancel{E}_T sample only), and the luminosity measurement.

Since the underlying graviton production mechanism is equivalent for both final states, the combination of the independent limits obtained from the two candidate samples is based on the predicted relative contributions of the four graviton production processes. Systematic uncertainties on the signal acceptances are treated as 100% correlated, while uncertainties on background estimates, obtained in most cases from data, are considered to be

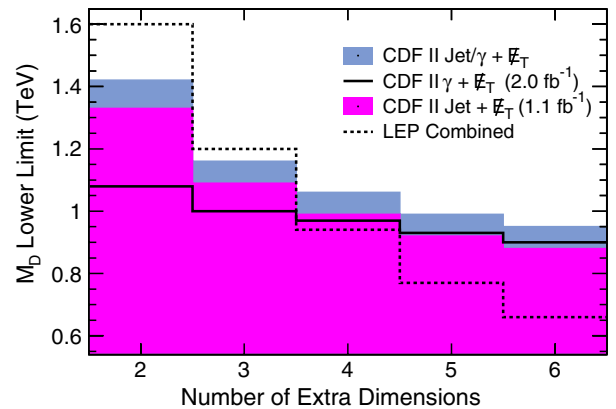


FIG. 3 (color online). 95% C.L. lower limits on M_D in the ADD model as a function of the number of extra dimensions in the model.

uncorrelated. The 95% C.L. lower limits on M_D from each candidate sample and the combined limits are given in Table III and plotted with LEP limits [17] in Fig. 3.

In conclusion, the CDF experiment has recently completed searches for new physics in the $\gamma + \cancel{E}_T$ and jet + \cancel{E}_T final states using data corresponding to 2.0 and 1.1 fb⁻¹ of integrated luminosity, respectively. The observed number of events is consistent with the expected background in both channels, and we place limits on the ADD model of LED that are the world's best for the cases of four or more extra dimensions.

We thank the Fermilab staff and the technical staffs of the participating institutions for their vital contributions. This work was supported by the U.S. Department of Energy and National Science Foundation; the Italian Istituto Nazionale di Fisica Nucleare; the Ministry of Education, Culture, Sports, Science and Technology of Japan; the Natural Sciences and Engineering Research Council of Canada; the National Science Council of the Republic of China; the Swiss National Science Foundation; the A.P. Sloan Foundation; the Bundesministerium für Bildung und Forschung, Germany; the Korean Science and Engineering Foundation and the Korean Research Foundation; the Science and Technology Facilities Council and the Royal Society, U.K.; the Institut National de Physique Nucleaire et Physique des Particules/CNRS; the Russian Foundation for Basic Research; the Ministerio de Educación y Ciencia and Programa Consolider-Ingenio 2010, Spain; the Slovak R&D Agency; and the Academy of Finland.

^aDeceased.

^bVisitor from Universiteit Antwerpen, B-2610 Antwerp, Belgium.

^cVisitor from Chinese Academy of Sciences, Beijing 100864, China.

^dVisitor from University of Bristol, Bristol BS8 1TL, United Kingdom.

^eVisitor from University of California Irvine, Irvine, CA 92697, USA.

^fVisitor from University of California Santa Cruz, Santa Cruz, CA 95064, USA.

^gVisitor from Cornell University, Ithaca, NY 14853, USA.

^hVisitor from University of Cyprus, Nicosia CY-1678, Cyprus.

ⁱVisitor from University College Dublin, Dublin 4, Ireland.

^jVisitor from University of Edinburgh, Edinburgh EH9 3JZ, United Kingdom.

^kVisitor from Universidad Iberoamericana, Mexico D.F., Mexico.

^lVisitor from University of Manchester, Manchester M13 9PL, United Kingdom.

^mVisitor from Nagasaki Institute of Applied Science, Nagasaki, Japan.

ⁿVisitor from University de Oviedo, E-33007 Oviedo, Spain.

^oVisitor from Queen Mary, University of London, London, E1 4NS, United Kingdom.

^pVisitor from Texas Tech University, Lubbock, TX 79409, USA.

^qVisitor from IFIC(CSIC-Universitat de Valencia), 46071 Valencia, Spain.

^rVisitor from Royal Society of Edinburgh, Edinburgh, EH2 2PQ, United Kingdom.

^sVisitor from Istituto Nazionale di Fisica Nucleare, Sezione di Cagliari, 09042 Monserrato (Cagliari), Italy.

- [1] N. Arkani-Hamed, S. Dimopoulos, and G. Dvali, Phys. Lett. B **429**, 263 (1998); Phys. Rev. D **59**, 086004 (1999).
- [2] G.F. Giudice, R. Rattazzi, and J.D. Wells, Nucl. Phys. B **544**, 3 (1999).
- [3] Jets are reconstructed over the full pseudorapidity coverage of the calorimeters ($|\eta| < 3.6$) using a fixed cone algorithm and cone sizes $\Delta R = \sqrt{(\Delta\phi)^2 + (\Delta\eta)^2}$ of 0.4 and 0.7 for $\gamma + \cancel{E}_T$ and jet + \cancel{E}_T events, respectively.
- [4] We use a coordinate system where θ is the polar angle to the proton beam, ϕ is the azimuthal angle about the beam axis, and η is the pseudorapidity defined as $-\text{Intan}(\theta/2)$. Missing transverse energy \cancel{E}_T is defined as $-\sum_i E_T^i \hat{n}^i$, where \hat{n}^i is a unit vector in the azimuthal plane from the beam line to the i th calorimeter tower.
- [5] A. Abulencia *et al.* (CDF Collaboration), Phys. Rev. Lett. **97**, 171802 (2006).
- [6] V.M. Abazov *et al.* (D0 Collaboration), Phys. Rev. Lett. **101**, 011601 (2008).
- [7] M. Goncharov *et al.*, Nucl. Instrum. Methods Phys. Res., Sect. A **565**, 543 (2006).
- [8] D. Acosta *et al.* (CDF Collaboration), Phys. Rev. D **71**, 032001 (2005).
- [9] F. Abe *et al.* (CDF Collaboration), Phys. Rev. D **52**, 4784 (1995) contains electromagnetic cluster and photon identification variable definitions.
- [10] F. Abe *et al.* (CDF Collaboration), Phys. Rev. Lett. **81**, 1791 (1998) contains standard photon identification criteria. The $\chi^2_{CES} < 20$ requirement is inefficient for photons incident at large angles relative to the detector face and therefore not used in selecting our $\gamma + \cancel{E}_T$ event sample.
- [11] We use a relevance vector machine trained on data to distinguish between collision and cosmic photon candidates; see C.C. Chang and C.J. Lin, <http://www.csie.ntu.edu.tw/~cjlin/libsvm>.
- [12] U. Baur, T. Han, and J. Ohnemus, Phys. Rev. D **57**, 2823 (1998).
- [13] T. Aaltonen *et al.* (CDF Collaboration), Phys. Rev. D **78**, 032015 (2008).
- [14] T. Sjöstrand *et al.*, Comput. Phys. Commun. **135**, 238 (2001).
- [15] R. Brun *et al.*, CERN Report No. CERN-DD/EE/84-1, 1987.
- [16] J. Conway, CERN Yellow Book Report No. CERN 2000-005, 2000, p. 247.
- [17] S. Ask, in *Proceedings of 32nd International Conference on High Energy Physics (ICHEP 2004)* (World Scientific, Singapore, 2005), Vol. 2, p. 1289.